Priya Gulial, Pankaj Thakur[*]

SAFETY ANALYSIS IN AN ELASTOPLASTIC ORTHOTROPIC ROTATING CYLINDER UNDER STEADY STATE TEMPERATURE

ANALIZA SIGURNOSTI ELASTOPLASTIČNOG ORTOTROPNOG ROTIRAJUĆEG CILINDRA SA STACIONARNOM TEMPERATUROM

Originalni naučni rad / Original scientific paper
Rad primljen / Paper received: 15.12.2023
https://doi.org/10.69644/ivk-2024-03-0309

Adresa autora / Author's address:
Department of Mathematics, ICFAI University, Himachal Pradesh, India P. Gulial 0009-0009-0266-2298; P. Thakur 0000-0001-8119-2697, *email: pankaj_thakur15@yahoo.co.in

Keywords
- stress
- cylinder
- angular speed
- isotropic
- orthotropic

Abstract

This research paper deals with the study of thermo-elastoplastic stress deformation in a rotating cylinder made of orthotropic material. The transition theory is applied to determining the presiding equation. An analytical solution for the rotating cylinder made of orthotropic material is presented. The behaviour of temperature, angular speed, and stress distribution are explored. The circumferential stress is maximal at the inner portion of the cylinder made of barite or copper material. With the introduction of thermal conditions, angular speed increases in the internal surface of barite material and decreases in that of copper material.

Ključne reči
- napon
- cilindar
- ugaona brzina
- izotropan
- ortotropan

Izvod

U ovom radu se istražuju deformacije usled termo-elastoplastičnih napona u rotirajućem cilindru od ortotropnog materijala. Primenjena je teorija prelaznih napona za određivanje odgovarajuće jednačine. Predstavljeno je analitičko rešenje za rotirajući cilindar od ortotropnog materijala. Istraženo je ponašanje temperature, ugaone brzine, kao i raspodela napona. Cirkularni napon ima maksimalnu vrednost u unutrašnjoj oblasti cilindra izrađenog od barita ili bakra. Uvođenjem termičkih uslova, ugaona brzina se povećava na unutrašnjoj površini za materijal barit, a opada kada je materijal bakar.

INTRODUCTION

Rotating cylinders have vast applications in engineering, such as ship propulsion systems, high-lift components such as aerofoils, and wind-driven devices. It is becoming increasingly less desirable to restrict design to the traditional elastic regime only due to the growing shortage of materials worldwide and their increased costs. Thick-walled cylindrical cross sections are commonly employed as pressure vessels to store industrial gases or transport high-pressure fluids. The elastoplastic deformation in a rotating cylinder was investigated by Hodge et al. /1/ by neglecting elastic and plastic strain hardening. Afterward, Bhatnagar et al. /2/ solved the problem for orthotropic cylinders. Zhao et al. /3/ explored techniques for finding stress deformation in thick-walled cylinders with distinct material parameters. It is found that for deformation, the value of strain energy depends on the initial or final geometry and also satisfies the boundary conditions. Additionally, Thakur /4/ examined the distribution of elastic-plastic thermal stresses in a rotating cylinder-formed isotropic material. Furthermore, Thakur et al. /5, 6/ have investigated thermo-elastoplastic and creep analysis in a spherical shell and cylinder with axial load and pressure of orthotropic material. Moreover, the elastoplastic analysis of a cylinder with a shaft under loading and unloading conditions was investigated by Prokudin /7/. Moreover, Temesgen et al. /8/ examined thermal stress deformation in a functionally graded thick-walled rotating cylinder with uniform pressure. The purpose of this research article is to investigate safety analysis in an elastoplastic orthotropic rotating cylinder under steady-state temperature using a generalised strain measure.

BASICS EQUATION

Let us consider a thick-walled cylinder made of orthotropic (e.g., barite) and isotropic (e.g., copper) material, having inner and outer radii a and b, which is rotating about its own axis with angular speed. Let steady-state temperature be applied to the inner surface at $r = a$.

In cylindrical coordinates, the displacement components are given by Seth, /9/:

$$u_1 = r(1-\xi),\ u_2 = 0,\ u_3 = dz\,. \tag{1}$$

Seth /10/ has given generalized components of strain as:

$$\varepsilon_{rr} = \frac{1}{m}\left[1-(r\xi'+\xi)^m\right],\quad \varepsilon_{\theta\theta} = \frac{1}{m}\left[1-\xi^m\right],$$
$$\varepsilon_{zz} = \frac{1}{m}\left[1-(1-d)^m\right],\quad \varepsilon_{r\theta} = \varepsilon_{\theta z} = \varepsilon_{zr} = 0\,, \tag{2}$$

where: $r\xi' = \xi P$.

The stress-strain relation is given by Thakur et al. /4/:

$$\tau_{rr} = \frac{c_{11}}{m}\left[1-(r\xi'+\xi)^m\right] + \frac{c_{12}}{m}\left[1-\xi^m\right] + \frac{c_{13}}{m}\left[1-(1-d)^m\right] - \alpha_1\Theta$$
$$\tau_{\theta\theta} = \frac{c_{21}}{m}\left[1-(r\xi'+\xi)^m\right] + \frac{c_{22}}{m}\left[1-\xi^m\right] + \frac{c_{23}}{m}\left[1-(1-d)^m\right] - \alpha_2\Theta$$
$$\tau_{zz} = \frac{c_{31}}{m}\left[1-(r\xi'+\xi)^m\right] + \frac{c_{32}}{m}\left[1-\xi^m\right] + \frac{c_{33}}{m}\left[1-(1-d)^m\right] - \alpha_3\Theta$$
$$\tau_{r\theta} = \tau_{\theta z} = \tau_{zr} = 0\,. \tag{3}$$

Equilibrium equation is:

$$\frac{d}{dr}(r\tau_{rr})-\tau_{\theta\theta}+\rho\omega^2 r^2=0\,. \tag{4}$$

Transition points: inserting Eq.(3) into Eq.(4), we get:

$$\xi P(1+P)^{m-1}\frac{dP}{d\xi}+P(P+1)^m+\frac{c_{12}}{c_{11}}P-\frac{1}{mc_{11}\xi^m}\times$$
$$\times\Big[(c_{11}-c_{21})\left\{1-\xi^m(P+1)^m\right\}+(c_{12}-c_{22})(1-\xi^m)+$$
$$+(c_{13}-c_{23})\left[1-(1-d)^m\right]\Big]-\frac{\rho\omega^2 r^2}{c_{11}\xi^m}=0\,. \tag{5}$$

The turning points ξ in Eq.(5) are $P\to\pm\infty$ (elastic to plastic state) and $P\to-1$ (plastic to creep state) by Seth /9, 10/. The boundary conditions are taken as:

$$\tau_{rr}=0 \text{ and } \Theta=\Theta_0 \text{ at } r=a\,,$$
$$\tau_{rr}=0 \text{ and } \Theta=0 \text{ at } r=b\,, \tag{6}$$

and $$\Theta=\frac{\Theta_0\ln(r/b)}{\ln(a/b)}\,.$$

Also, $$\int_a^b r\tau_{zz}\,dr=0\,. \tag{7}$$

SOLUTION

Let the transition function ζ be taken as Thakur et al. /4-6, 11-21/ and Seth /9, 10/:

$$\zeta=1-\frac{m}{(c_{11}+c_{12}+c_{13})}\left[\tau_{rr}-\frac{m\rho\omega^2r^2}{2}\right]\cong\frac{1}{(c_{11}+c_{12}+c_{13})}\times$$
$$\times\left[c_{11}\xi^m(P+1)^m+c_{12}\xi^m+c_{13}(1-d)^m\frac{m\rho\omega^2r^2}{2}\right]. \tag{8}$$

By taking logarithmic differentiations and the transition point Eq.(8), the transition function is given:

$$R=Ar^{-k_1}\,, \tag{9}$$

where: $k_1=(c_{11}-c_{21})/c_{11}$.

From Eqs. (8) and (9), the radial stress is given:

$$\tau_r=\frac{c_{11}+c_{12}+c_{13}}{m}\left[1-Ar^{-k_1}\right]-k_1\alpha_1\Theta-\frac{\rho\omega^2r^2}{2}\,. \tag{10}$$

Using Eq.(6) into Eq.(10), we get:

$$A=\frac{2k_1\alpha_1\Theta_0+\rho\omega^2(a^2-b^2)}{\rho\omega^2(a^2b^{-k_1}-b^2a^{-k_1})+2k_1\alpha_1\Theta_0b^{-k_1}}$$
$$\frac{c_{11}+c_{12}+c_{13}}{m}=\frac{\rho\omega^2(a^2b^{-k_1}-b^2a^{-k_1})+2k_1\alpha_1\Theta_0b^{-k_1}}{2(b^{-k_1}-a^{-k_1})}\,. \tag{11}$$

Substituting Eq.(11) into Eq.(10), we get:

$$\tau_r=\frac{\rho\omega^2b^2\left[R_0^2(1-R^{-k_1})+R^2(R_0^{-k_1}-1)+R^{-k_1}-R_0^{-k_1}\right]}{2(1-R_0^{-k_1})}+$$
$$+\beta_0k_1\left[\frac{1-R^{-k_1}}{1-R_0^{-k_1}}-\frac{\ln R}{\ln R_0}\right]. \tag{12}$$

Inserting Eq.(12) into Eq.(4), we get:

$$\tau_\theta=\tau_r+\frac{\rho\omega^2b^2k_1R^{-k_1}(R_0^2-1)+2k_1^2\beta_0R^{-k_1}}{2(1-R_0^{-k_1})}-\frac{\beta_0k_1}{\ln R_0}\,. \tag{13}$$

Using Eq.(7) and the third equation of Eq.(3), we get:

$$\tau_{zz}=k_2\left[(\tau_r+\tau_\theta)-\frac{\rho\omega^2b^2}{2}(1+R_0^2)\right]+\frac{\beta_0}{\ln R_0}\left[\left(1+\frac{\alpha_2}{\alpha_1}\right)k_2-\frac{\alpha_3}{\alpha_1}\right]\times$$
$$\times\left\{\ln R-\frac{2}{(1-R_0^2)}\left(\frac{R_0^2}{4}-\frac{1}{4}-\frac{R_0^2}{2}\ln R_0\right)\right\}, \tag{14}$$

where: $R_0=a/b$; $R=r/b$; $\beta_0=\alpha_1\Theta_0$, and $k_2=c_{32}/(c_{12}+c_{22})$.

Equation (13) gives:

$$\tau_\theta-\tau_r=-\frac{\rho\omega^2b^2}{2}k_1R_0^{-k_1}\left[\frac{R_0^2-1}{1-R_0^{-k_1}}\right]+k_1\beta_0\left[\frac{k_1R^{-k_1}}{(1-R_0^{-k_1})}+\frac{1}{\ln R_0}\right] \tag{15}$$

From Eq.(15), $|\tau_{\theta\theta}-\tau_{rr}|$ has a maximum value at $R=R_0$, therefore, yielding will be given as:

$$\left|\tau_\theta-\tau_r\right|_{R=R_0}=\left|-\frac{\rho\omega^2b^2}{2}k_1R_0^{-k_1}\left[\frac{R_0^2-1}{1-R_0^{-k_1}}\right]+k_1\beta_0\left[\frac{k_1R_0^{-k_1}}{(1-R_0^{-k_1})}+\frac{1}{\ln R_0}\right]\right|=Y$$

and angular speed for the initial yielding surface becomes:

$$\Omega^2_{\text{inital yielding}}=\frac{\rho\omega^2b^2}{Y}=\left|\frac{2(1-R_0^{-k_1})}{k_1R_0^{-k_1}(R_0^2-1)}\right|\left[1-k_1\beta_1\left|\frac{k_1R_0^{-k_1}}{(1-R_0^{-k_1})}+\frac{1}{\ln R_0}\right|\right] \tag{16}$$

where: $\beta_1=\beta_0/Y$.

The non-dimensional stresses for the initial yielding surface, Eqs.(12)-(14), become:

$$\sigma_\theta=\sigma_r+\frac{\Omega^2_{\text{inital yielding}}k_1R^{-k_1}(R_0^2-1)}{2(1-R_0^{-k_1})}+\beta_1k_1\left[\frac{k_1R^{-k_1}}{1-R_0^{-k_1}}-\frac{1}{\ln R_0}\right],$$
$$\sigma_r=\frac{\Omega^2_{\text{inital yielding}}\left[R_0^2(1-R^{-k_1})+R^2(R_0^{-k_1}-1)+R^{-k_1}-R_0^{-k_1}\right]}{2(1-R_0^{-k_1})}+$$
$$+\beta_1k_1\left[\frac{1-R^{-k_1}}{1-R_0^{-k_1}}-\frac{\ln R}{\ln R_0}\right],$$
$$\sigma_z=k_4\left[(\sigma_r+\sigma_\theta)-\frac{\Omega^2_{\text{inital yielding}}}{2}(1+R_0^2)\right]+\frac{\beta_1}{\ln R_0}\left[(1+\beta_2)k_4-\beta_3\right]\times$$
$$\times\left\{\ln R-\frac{2}{(1-R_0^2)}\left(\frac{R_0^2}{4}-\frac{1}{4}-\frac{R_0^2}{2}\ln R_0\right)\right\}, \tag{17}$$

where: $\sigma_\theta=\tau_{\theta\theta}/Y$, $\sigma_r=\tau_{rr}/Y$, $\sigma_z=\tau_{zz}/Y$ and $\beta_3=\alpha_3/\alpha_1$.

SUBSEQUENT YIELDING SURFACE

For fully plastic surfaces, $c_{13}=c_{12}=c_{11}$, $c_{33}=c_{31}=c_{32}$ and $c_{23}=c_{21}=c_{22}$, Eqs.(16)-(17) become:

$$\sigma_\theta=\sigma_r+\frac{\Omega^2_{\text{fully plastic}}k_5R^{-k_3}(R_0^2-1)}{2(1-R_0^{-k_3})}+\beta_1k_3\left[\frac{k_5R^{-k_3}}{1-R_0^{-k_3}}-\frac{1}{\ln R_0}\right]$$
$$\sigma_r=\frac{\Omega^2_{\text{fully plastic}}\left[R_0^2(1-R^{-k_3})+R^2(R_0^{-k_3}-1)+R^{-k_3}-R_0^{-k_3}\right]}{2(1-R_0^{-k_3})}+$$
$$+\beta_1k_3\left[\frac{1-R^{-k_3}}{1-R_0^{-k_3}}-\frac{\ln R}{\ln R_0}\right],$$
$$\sigma_z=k_4\left[(\sigma_r+\sigma_\theta)-\frac{\Omega^2_{\text{inital yielding}}}{2}(1+R_0^2)\right]+\frac{\beta_1}{\ln R_0}\times$$
$$\times\left[(1+\beta_2)k_4-\beta_3\right]\left\{\ln R-\frac{2}{(1-R_0^2)}\left(\frac{R_0^2}{4}-\frac{1}{4}-\frac{R_0^2}{2}\ln R_0\right)\right\},$$

and

$$\Omega_{\text{fully plastic}} = \left|\frac{2(1-R_0^{-k_3})}{k_3 R_0^{-k_3}(R_0^2-1)}\right|\left[1-k_3\beta_1\left|\frac{k_5 R_0^{-k_3}}{(1-R_0^{-k_3})}+\frac{1}{\ln R_0}\right|\right] \quad (18)$$

where: $k_3 = (c_{11} - c_{22})/c_{11}$; and $k_4 = c_{22}/(c_{12} + c_{22})$.

ISOTROPIC MATERIALS

For isotropic material, the elastic constants are $c_{12} = c_{21} = c_{32} = c_{23} = c_{31} = c_{13} = c_{11} - 2c_{66}$, $\lambda = c_{12}$, $\mu = (c_{11} - c_{12})/2$, $c_{11} = c_{22} = c_{33}$, and $c = (c_{11} - c_{12})/c_{11}$. Eq.(18) becomes:

$$\sigma_\theta = \sigma_r + \frac{\Omega^2_{\text{isotropic initial}}\, cR^{-c}(R_0^2-1)}{2(1-R_0^{-c})} + \beta_1 c\left[\frac{cR^{-c}}{1-R_0^{-c}} - \frac{1}{\ln R_0}\right],$$

$$\sigma_r = \frac{\Omega^2_{\text{isotropic initial}}\left[R_0^2(1-R^{-c}) + R^2(R_0^{-c}-1) + R^{-c} - R_0^{-c}\right]}{2(1-R_0^{-c})} + \\ + \beta_1 c\left[\frac{1-R^{-c}}{1-R_0^{-c}} - \frac{\ln R}{\ln R_0}\right],$$

$$\sigma_z = \left(\frac{1-c}{2-c}\right)\left[(\sigma_r+\sigma_\theta) - \frac{\Omega^2_{\text{inital yielding}}}{2}(1+R_0^2)\right] + \frac{\beta_1}{\ln R_0}\times \\ \times\left[(1+\beta_2)\left(\frac{1-c}{2-c}\right) - \beta_3\right]\left\{\ln R - \frac{2}{(1-R_0^2)}\left(\frac{R_0^2}{4} - \frac{1}{4} - \frac{R_0^2}{2}\ln R_0\right)\right\},$$

and
$$\Omega^2_{\text{isotropic initial}} = \left|\frac{2(1-R_0^{-c})}{cR_0^{-c}(R_0^2-1)}\right|\left[1-c\beta_1\left|\frac{cR_0^{-c}}{(1-R_0^{-c})} + \frac{1}{\ln R_0}\right|\right] \quad (19)$$

The fully-plastic surface, Eq.(19), becomes:

$$\sigma_\theta = \sigma_r + \frac{\Omega^2_{\text{isotropic fully-plastic}}(R_0^2-1)}{2\ln R_0} - \frac{\beta_1}{\ln R_0},$$

$$\sigma_r = \frac{\Omega^2_{\text{isotropic fully-plastic}}}{2}\left[(1-R^2) + (R_0^2+1)\frac{\ln R}{\ln R_0} - \beta_1 \ln R\right],$$

$$\sigma_z = \frac{1}{2}\left[(\sigma_r+\sigma_\theta) - \frac{\Omega^2_{\text{isotropic fully-plastic}}}{2}(1+R_0^2)\right] + \frac{\beta_1}{\ln R_0}\left[\frac{1+\beta_2}{2} - \beta_3\right]\times \\ \times\left\{\ln R - \frac{2}{(1-R_0^2)}\left(\frac{R_0^2}{4} - \frac{1}{4} - \frac{R_0^2}{2}\ln R_0\right)\right\},$$

and
$$\Omega^2_{\text{isotropic fully-plastic}} = \left|\frac{2\ln R_0}{R_0^2-1}\right|\left[\left|\ln R_0\right| - \frac{\beta_1}{\left|\ln R_0\right|}\right]. \quad (20)$$

VALIDATION OF RESULTS

The present results from Eqs.(19)-(20) are the same by neglecting thermal conditions compared to the results given by Thakur et al. /4/.

DISCUSSION

To emphasize the above, we have taken the following values of c_{ij} (units of 1010 N/m^2): $c_{11} = 0.891$, $c_{12} = 0.46$, $c_{21} = 0.4614$, $c_{22} = 0.7842$, $c_{32} = 0.2676$ for orthotropic material /6/ (e.g., barite); $c = 0.5$ for isotropic material /6/ (e.g., copper). Figure 1 clearly manifests that a cylinder made of barite requires higher values of angular speed at the inner surface for the initial, fully plastic state as compared to copper. Figure 2 depicts that a cylinder made of barite needs a higher value of angular speed at the inner portion in comparison to a cylinder made of copper in its initial, fully plastic state. With the addition of the thermal effect, angular speed must increase at the inner portion of a cylinder made of orthotropic material and decrease for isotropic material.

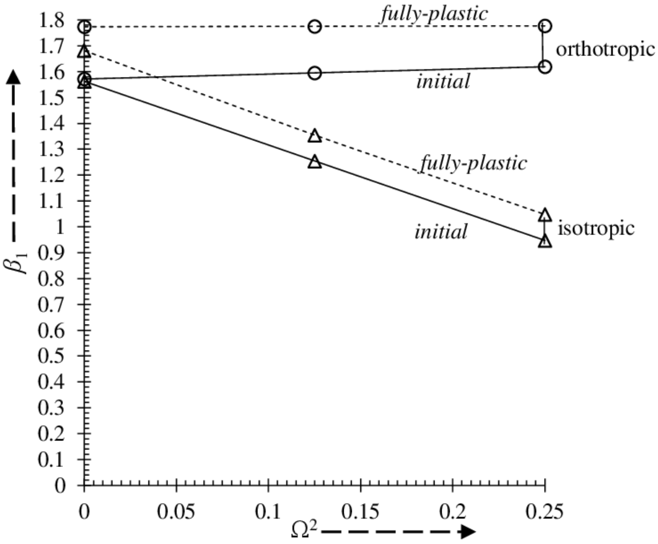

Figure 1. Graph between β_1 vs. Ω^2.

Figure 3 depicts that circumferential stress is maximum at the inner portion of the cylinder made of barite or copper. Moreover, the rotating cylinder made of isotropic material must need more circumferential or axial stress in comparison to the cylinder made of orthotropic material, and the imposed boundary conditions eliminate the radial stress on the internal or external surface.

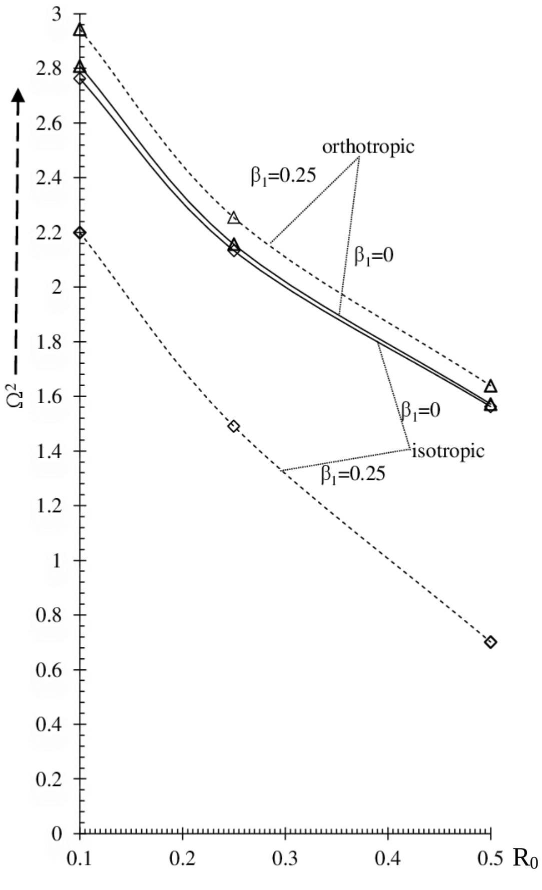

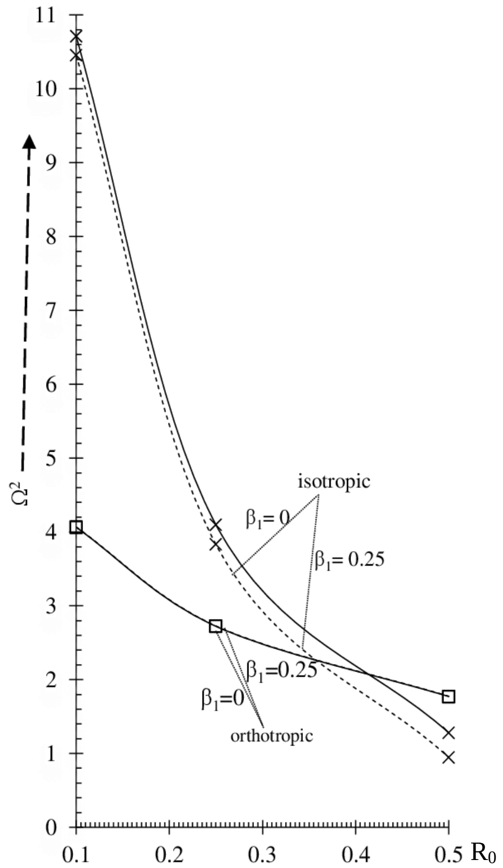

Figure 2. Graph between Ω^2 vs. R_0.

CONCLUSION

The main findings are given as follows:
- the cylinder made of orthotropic material needs more angular speed in the inner portion;
- by effect of thermal conditions, angular speed increases in the internal surface of barite material and decreases in that of copper material;
- the circumferential stress is maximum at the inner portion of the cylinder made of barite or copper material;
- the cylinder of barite material is more convenient than that of copper material.

ACKNOWLEDGEMENTS

This research article is especially dedicated to Prof. Dr. Aleksandar Sedmak (editor-in-chief Emeritus), to Prof. Dr. Zoran Radaković (editor-in-chief) of *Structural Integrity and Life* journal, and to the publishers: the Society for Structural Integrity and Life 'Prof. Dr. Stojan Sedmak', and the IMS Institute, in Belgrade, Serbia.

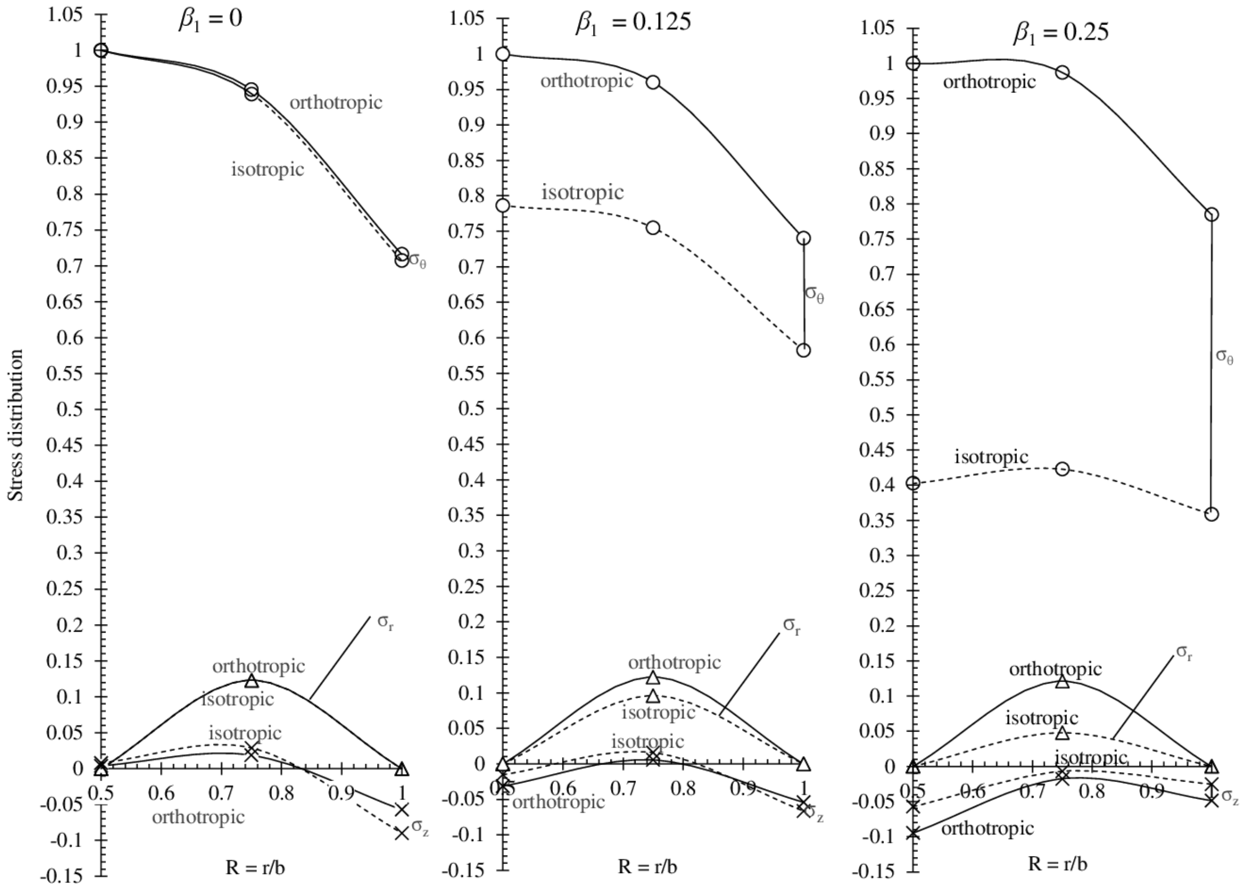

Figure 3. Stress distribution and displacement vs. radius.

Abbreviations

a - outer radius
b - inner radius
α_1, α_2 α_3 - thermal expansion coefficients
d' - constant
Y - yielding stress
ξ - variable in term of r
r, θ, z - polar co-ordinates
c - compressibility factor
r - variable in terms of x, y and z
R_0, R - radii ratio
c_{ij} - elastic constants
A - constant of integration
Ω_2 - speed factor (dimensionless)
ρ - density
ω - angular velocity
σ_r, σ_θ, σ_z - radial, circumferential, axial stress components

REFERENCES

1. Hodge Jr., P.G., Balaban, M. (1962), *Elastic-plastic analysis of a rotating cylinder*, Int. J Mech. Sci. 4(6): 465-476. doi: 10.1016/S0020-7403(62)80008-3
2. Bhatnagar, N.S., Gupta, S.K. (1969), *Analysis of thick-walled orthotropic cylinder in the theory of creep*, J Phys. Soc. Jpn. 27(6): 1655-1661. doi: 10.1143/JPSJ.27.1655
3. Zhao, W., Seshadri, R. Dubey, R.N. (2003), *On thick-walled cylinder under internal pressure*, J Pres. Ves. Technol. 125(3): 267-273. doi: 10.1115/1.1593082
4. Thakur, P. (2011), *Elastic-plastic transition stresses in rotating cylinder by finite deformation under steady-state temperature*, Therm. Sci. 15(2): 537-543. doi: 10.2298/TSCI1102537P
5. Thakur, P. (2013), *Creep transitional stresses of orthotropic thick-walled cylinder under combined axial load under internal pressure*, Facta Universitatis, Ser. Mech. Eng. 11(1): 13-18.
6. Thakur, P., Sethi M. (2020), *Elastoplastic deformation in an orthotropic spherical shell subjected to temperature gradient*, Math. Mech. Solids, 25(1): 26-34. doi: 10.1177/1081286519857128
7. Prokudin A.N. (2020), *Exact elastoplastic analysis of a rotating cylinder with a rigid inclusion under mechanical loading and unloading*, J Appl. Math. Mech. (ZAMM), 100(3): e201900213. doi: 10.1002/zamm.201900213
8. Temesgen, A.G., Singh, S.B., Thakur, P. (2021), *Elastoplastic analysis in functionally graded thick-walled rotating transversely isotropic cylinder under a radial temperature gradient and uniform pressure*, Math. Mech. Solids, 26(1): 5-17. doi: 10.1177/1081286520934041
9. Seth, B.R. (1962), *Transition theory of elastic-plastic deformation, creep and relaxation*, Nature, 195: 896-897. doi:10.1038/195896a0.
10. Seth, B.R. (1966), *Measure-concept in mechanics*, Int. J Non-Linear Mech. 1(1): 35-40. doi: 10.1016/0020-7462(66)90016-3
11. Sethi, M., Thakur, P., Singh, H.P. (2019), *Characterization of material in a rotating disc subjected to thermal gradient by using Seth transition theory*, Struct. Integr. Life, 19(3): 151-156.
12. Thakur, P., Shahi, S., Singh, S.B., Sethi, M. (2019), *Elastic-plastic stress concentrations in orthotropic composite spherical shells subjected to internal pressure*, Struct. Integr. Life, 19(2): 73-77.
13. Thakur, P., Sethi, M. (2019), *Lebesgue measure in an elasto-plastic shell*, Struct. Integr. Life, 19(2): 115-120.
14. Thakur, P., Gupta, N., Gupta, K., Sethi, M. (2020), *Elastic-plastic transition in an orthotropic material disk*, Struct. Integr. Life, 20(2): 169-172.
15. Thakur, P., Chand, S., Sukhvinder, et al. (2020), *Density parameter in a transversely and isotropic disc material with rigid inclusion*, Struct. Integr. Life, 20(2): 159-164.
16. Thakur, P., Kumar, N., Sukhvinder (2020), *Elasto-plastic density variation in a deformable disk*, Struct. Integr. Life, 20 (1): 27-32.
17. Kumar, N., Thakur, P. (2021), *Thermal behaviour in a rotating disc made of transversely isotropic material with rigid shaft*, Struct. Integr. Life, 21(3): 217-223.
18. Kumar, A., Sood, S., Thakur, P., Kumar, N. (2022), *Safety analysis in an isotropic material disc fitted with a rigid shaft subjected to thermo-mechanical load by using transition theory*, Struct. Integr. Life, 22(2): 193-201.
19. Kumar, N., Thakur, P. (2022), *Behaviour of creep stress and strain rates in a solid disc made of isotropic material with thermal condition*, Struct. Integr. Life, 22(2): 202-209.
20. Chand, S., Sood, S., Thakur, P., Gupta, K. (2023), *Elastoplastic stress deformation in an annular disk made of isotropic material and subjected to uniform pressure*, Struct. Integr. Life, 23(1): 61-64.
21. Singh, N., Kaur, J., Thakur, P., Murali, G. (2023), *Structural behaviour of annular isotropic disk made of steel/copper material with gradually varying thickness subjected to internal pressure*, Struct. Integr. Life, 23(3): 293-297.